Neurobiology of Disease 134 (2020) 104679

Contents lists available at ScienceDirect

Neurobiology of Disease

journal homepage: www.elsevier.com/locate/ynbdi

A randomized, double-blind, placebo-controlled trial of blue wavelength light exposure on sleep and recovery of brain structure, function, and cognition following mild traumatic brain injury

William D.S. Killgore*, John R. Vanuk, Bradley R. Shane, Mareen Weber, Sahil Bajaj

Department of Psychiatry, College of Medicine, University of Arizona, United States of America

ARTICLE INFO

Keywords:
mTBI
Concussion
Light therapy
Blue light
Sleep
Circadian rhythm
Neuroimaging
DTI
VBM
Connectivity

ABSTRACT

Sleep and circadian rhythms are among the most powerful but least understood contributors to cognitive performance and brain health. Here we capitalize on the circadian resetting effect of blue-wavelength light to phase shift the sleep patterns of adult patients (aged 18–48 years) recovering from mild traumatic brain injury (mTBI), with the aim of facilitating recovery of brain structure, connectivity, and cognitive performance. During a randomized, double-blind, placebo-controlled trial of 32 adults with a recent mTBI, we compared 6-weeks of daily 30-min pulses of blue light (peak λ = 469 nm) each morning versus amber placebo light (peak λ = 578 nm) on neurocognitive and neuroimaging outcomes, including gray matter volume (GMV), resting-state functional connectivity, directed connectivity using Granger causality, and white matter integrity using diffusion tensor imaging (DTI). Relative to placebo, morning blue light led to phase-advanced sleep timing, reduced daytime sleepiness, and improved executive functioning, and was associated with increased volume of the posterior thalamus (i.e., pulvinar), greater thalamo-cortical functional connectivity, and increased axonal integrity of these pathways. These findings provide insight into the contributions of the circadian and sleep systems in brain repair and lay the groundwork for interventions targeting the retinohypothalamic system to facilitate injury recovery.

1. Introduction

Sleep and circadian rhythms have potent effects on human health, neurobiology, and cognitive functioning. Without the benefit of restorative sleep, elementary cognitive performance declines rapidly and is accompanied by unpredictable lapses of attention (Durmer and Dinges, 2005), and impairments in higher-order cognitive capacities such as judgment, decision-making, and executive functions (Killgore et al., 2006; Killgore et al., 2007; Tucker et al., 2010). At the neural level, sleep is critical for processes that facilitate physiological maintenance and repair, including flushing out accumulated neurotoxins (Xie et al., 2013), restoration of damaged DNA in neurons (Bellesi et al., 2016), production of oligodendrocyte precursor cells involved in myelin formation (Bellesi et al., 2013), sustainment of myelin sheath thickness (Bellesi et al., 2018), and maintaining the structural plasticity and homeostasis of synaptic connections (de Vivo et al., 2017; Tononi and Cirelli, 2014). Animal models demonstrate that sleep plays a vital role in recovery from brain injury (Gao et al., 2010; Zunzunegui et al., 2011), presumably through many of the mechanisms just described. Clearly, one of the many functions of sleep is to facilitate repair and restoration of brain systems that have been damaged, depleted, or degraded. Sleep, however, is not driven solely by homeostatic forces; our propensity for sleep is inextricably linked with the diurnal circadian rhythm of melatonin secretion by the pineal gland and the attendant fluctuations in alertness. Because retinal light exposure suppresses melatonin, circulating levels of this hormone are nearly absent throughout the circadian day, but typically rise dramatically as light levels decline in the evening (Cajochen et al., 2003). For humans, the most efficient, restful, and restorative sleep occurs when the sleep cycle is closely aligned with the circadian night (Arendt, 2006; Lavie, 2001).

Circadian rhythms are demonstrated by almost every cell within the human body, comprising a hierarchical multi-oscillator system that is regulated by the suprachiasmatic nucleus (SCN) of the hypothalamus (Honma, 2018). The near 24-hour rhythm of this system is maintained by a molecular entrainment process that resets the circadian clock each period via retinal exposure to light. When light strikes the retina, it

* Corresponding author.
E-mail address: killgore@psychiatry.arizona.edu (W.D.S. Killgore).

https://doi.org/10.1016/j.nbd.2019.104679
Received 10 July 2019; Received in revised form 20 October 2019; Accepted 15 November 2019
Available online 18 November 2019

stimulates melanopsin-based intrinsically photosensitive retinal ganglion cells (ipRGCs) that are uniquely sensitive to wavelengths in the blue range of the light spectrum (Panda et al., 2005; Provencio et al., 2000; Qiu et al., 2005). These ipRGCs project extensively, via the retinohypothalamic tract (RHT), to the SCN (Hattar et al., 2002; Panda et al., 2002), which in turn, suppresses the production of melatonin by the pineal gland (Sapede and Cau, 2013). Thus, exposure to blue wavelength light in the morning suppresses melatonin and phase advances the circadian rhythm (i.e., sleep onset occurs earlier in the next period) while similar exposure in the evening leads to a phase delay (i.e., sleep onset will be pushed back later in the next period). This modifiability of the circadian rhythm by light exposure has led to recent efforts to use targeted phototherapy to treat circadian-related sleep problems.

While many types of sleep difficulties could potentially benefit from light exposure interventions, one disorder where sleep may play a key role in brain repair and recovery is mild traumatic brain injury (mTBI) (Raikes and Killgore, 2018). Approximately 50% of patients with an mTBI experience chronic sleep disruption and associated cognitive decrements following injury (Orff et al., 2009; Rao et al., 2008; Verma et al., 2007). Critically, mTBI is associated with disturbances in the normal rhythm of melatonin production (Grima et al., 2016; Shekleton et al., 2010). As melatonin production in the evening plays a crucial role in regulating sleep onset, disruptions in this cycle can have pronounced effects on sleep quality (Grima et al., 2016; Shekleton et al., 2010). Moreover, sleep problems following an mTBI are associated with worse cognitive recovery and greater neuropsychiatric complications (Gilbert et al., 2015; Sullivan et al., 2016). Based on the aforementioned role of sleep in neural maintenance and repair, sleep disturbance in mTBI may hinder normal brain recovery following an injury. We, therefore, proposed to facilitate recovery from an mTBI by optimizing the timing and quality of sleep via targeted light exposure, which has not been directly assessed through experimental research. Sinclair and colleagues first demonstrated that morning blue-wavelength light exposure was effective at reducing subjective fatigue and daytime sleepiness in patients recovering from TBI (Sinclair et al., 2014), however, objective outcomes were not measured. More recently, our team reported preliminary evidence that morning blue light exposure may be helpful in changing the water diffusion patterns of cerebral white matter in patients recovering from mTBI (Bajaj et al., 2017). However, full examination of the combined effects of blue light treatment on circadian timing, neurocognitive performance, and multimodal assessment of neural mechanisms has not been undertaken.

Here, we identified the cognitive and neurobiological changes produced by a 6-week intervention of daily morning blue-wavelength light exposure in individuals recovering from a non-complicated mTBI. In a randomized, double-blind, placebo-controlled trial, adults with a documented mTBI in the preceding 18 months used an LED lightbox each morning for 30-min. Each device was fitted with either BLUE or AMBER LEDs (see Fig. 1). Sleep/wake activity was monitored with wrist actigraphy and on-line sleep diaries for one week before treatment, and throughout the 6-week intervention period. Participants also completed a comprehensive neuropsychological assessment battery, a series of objective multiple sleep latency tests (MSLTs), and functional and structural magnetic resonance imaging (MRI) scans on the day preceding the treatment period and immediately upon completion of the intervention. We hypothesized that the blue light intervention would lead to a greater phase advance in the circadian rhythm, improved sleep, and enhanced daytime alertness relative to amber placebo. Further, we hypothesized that compared to the placebo condition, the blue light would produce greater improvement in neurocognitive performance and symptom reduction, which would correspond to increased functional and structural connectivity within brain networks involved in visual attention.

2. Methods

2.1. Participants

Individuals with a documented history of an mTBI in the preceding 18 months were recruited from the greater Boston Metropolitan area to participate. Interested volunteers first underwent a rigorous telephone screening interview, followed by a detailed in-person interview to determine eligibility. Volunteers were between the ages of 18 and 50 and had experienced a “concussion” or non-complicated mTBI within the preceding 18 months, but no sooner than 4 weeks prior to their initial assessment. Before participation, all individuals were required to provide written documentation by a medical or other relevant professional (e.g., physician, nurse, emergency medical technician, coach, physical trainer, police officer, security guard) who either witnessed or was involved in the immediate response to the injury. Eligible volunteers were required to meet the definition of an mTBI as specified by the VA/DoD practice guidelines (VA/DoD Management of Concussion/mTBI Working Group, 2009), which define an mTBI as a traumatically induced structural injury and/or physiological disruption caused by an external force (e.g., head impact, blast wave) leading to an alteration in mental status (e.g., confusion, disorientation, retrograde or anterograde amnesia), consciousness (i.e., loss of consciousness < 30 min; alteration of consciousness up to 24 h), or post-traumatic amnesia up to 24 h, and/or a Glasgow Coma Scale ≥ 13. For this study, all participants were also required to have reported the onset of significant sleep-related problems that emerged or worsened following the injury. Only primary English speakers (i.e., those who began speaking English as their primary language in the home by 3 years of age), and those who were right-handed according to the Edinburgh Handedness Inventory (Oldfield, 1971) were included. Potential volunteers were also excluded for any history of neurological, mood, or psychotic disorder that was present before the index traumatic injury, as well as abnormal visual acuity not correctable by contact lenses, metal within the body, pregnancy, or other contraindications for MRI. Other exclusionary criteria included current or anticipated shift work, intent to leave the time zone during the course of the study, use of contraindicated medications (i.e., sleep medications; medications that affect neuroimaging), or use of illicit substances, including recent or long-term marijuana use, or excessive alcohol use (as defined by CDC criteria). Prior to enrollment, all participants completed written informed consent, and were compensated for their time in the study. The protocol for this experiment was approved by the Institutional Review Boards (IRB) of Partners Health Care, McLean Hospital, and the U.S. Army Human Use Protections Office.

Primary endpoints for this study, collected at baseline and post-treatment, included 1) actigraphically measured sleep (minutes per night), 2) actigraphically measured circadian phase shift (i.e., shift in sleep onset time, wake time, and midpoint of the sleep period), and 3) subjective sleepiness, and 4) objective sleepiness. Secondary endpoints included 1) cognitive performance (i.e., psychomotor vigilance, neuropsychological performance, and executive functioning), 2) brain volumetrics, 3) functional connectivity, and 4) white matter axonal integrity. Each of these was assessed at the baseline week or visit and again during the final week or follow-up visit. A total of 38 participants met full criteria for initial enrollment in the study. However, due to participant non-compliance ($n = 2$), disqualifying psychopathology ($n = 1$), and claustrophobia upon entering the scanner ($n = 1$), 34 participants were ultimately randomized to one of the treatment groups (Fig. 2). Two participants in the BLUE condition failed to complete required study procedures during the course of treatment, yielding complete data for most outcome measures from 32 participants (15 male; 17 female) ranging in age from 18 to 48 years ($M = 23.27$; $SD = 7.14$). Of these participants, $n = 16$ (50%) received the active BLUE light condition and $n = 16$ (50%) received the placebo AMBER placebo light condition. Table 1 presents the demographic data for the

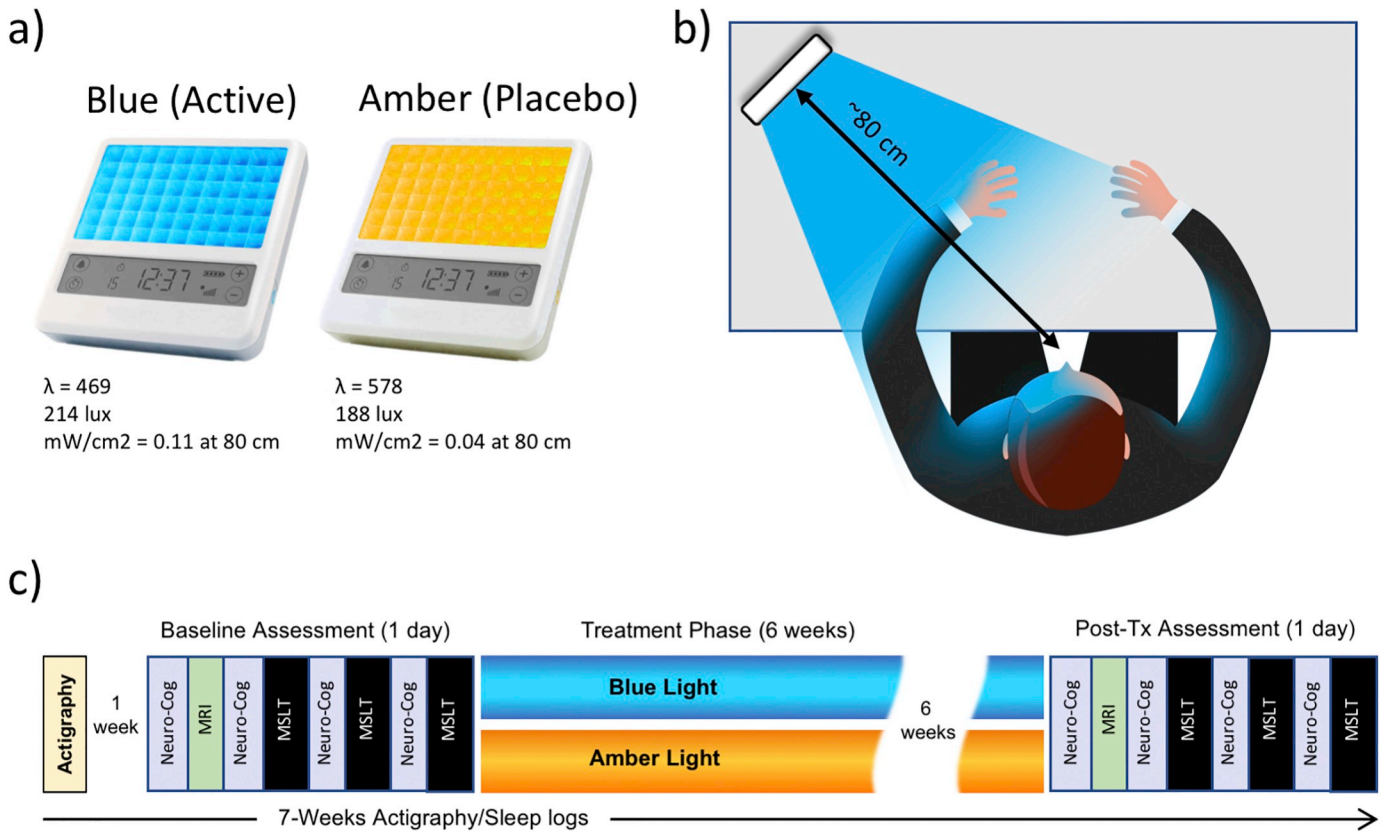

Fig. 1. Light therapy conditions and experimental design. (a) Participants received either a blue (active condition) or amber (placebo condition) light box fitted with light-emitting diodes. (b) The participant was instructed to place the device at arm"s length on a table at an approximately 45-degree angle and bathe their face with the light for 30-minutesmin each morning. (c) The study lasted for 7-weeks. The figure shows that the participant wore an actigraph sleep monitor for the entire study period. After one week of baseline actigraphy, the participant completed a full day of neurocognitive assessments, magnetic resonance imaging (MRI) scans, and multiple sleep latency tests (MSLTs). Participants were then randomized to one of the two light treatment conditions (blue versus amber), during which time they used the lightbox each morning. At the end of 6-weeks, participants returned to complete another day-long assesses session with the same measures collected at baseline. (For interpretation of the references to colour in this figure legend, the reader is referred to the web version of this article.)

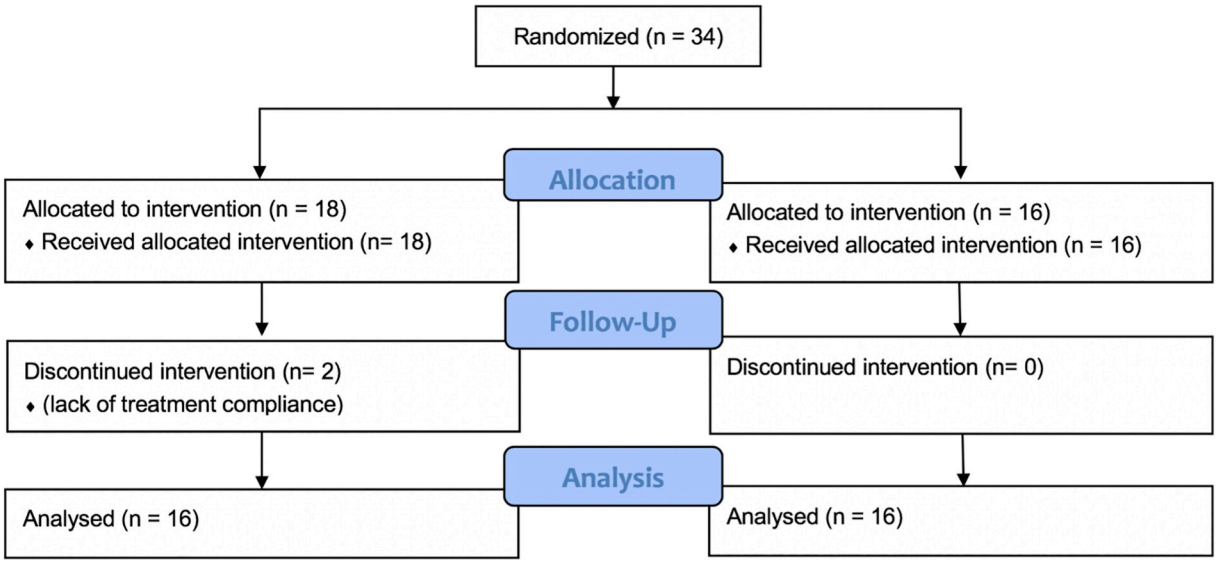

Fig. 2. Participant flow diagram. The figure shows that 3 participants were randomly assigned to either the active blue light condition or placebo amber light condition. Two participants from the blue group were excluded due to non-compliance, yielding 16 participants per group in the final analysis. (For interpretation of the references to colour in this figure legend, the reader is referred to the web version of this article.)

Table 1
Baseline demographics for blue and amber groups.

	Blue	Amber	Test	p-value
N	16 (50%)	16 (50%)		
Female	9 (56.2%)	8 (50%)	χ^2 (1) = 0.125	0.72
Male	7 (43.8%)	8 (50%)		
Age	23.2 (7.1)	23.3 (7.4)	$t(30) = 0.037$	0.97
Education	15.0 (2.4)	14.6 (2.2)	$t(30) = 0.466$	0.65
# Concussions	2.4 (1.8)	2.2 (1.6)	$t(30) = 0.368$	0.72
Months Since Injury	6.8 (4.4)	6.7 (3.6)	$t(30) = 0.066$	0.95
RPCSQ Total	13.6 (11.1)	16.7 (8.3)	$t(30) = 0.883$	0.38
NSI	18.4 (19.4)	16.9 (10.5)	$t(30) = 0.260$	0.80
BDI	7.3 (6.6)	7.1 (3.4)	$t(30) = 0.134$	0.89
FOSQ	16.1 (2.9)	16.5 (2.1)	$t(30) = 0.38$	0.71
MEQ	51.8 (4.3)	50.8 (6.5)	$t(30) = 0.514$	0.61

samples.

2.2. General procedure

Over seven weeks, participants completed three laboratory visits, including two full-day neurocognitive assessments plus neuroimaging scans, and were randomly assigned to complete a 6-week at-home light treatment regimen with either daily BLUE or AMBER light therapy each morning.

2.2.1. Visit 1: Intake

Upon arrival, each eligible participant completed the informed consent process followed by the Neurobehavioral Symptom Inventory (NSI) (King et al., 2012), and the MINI International Neuropsychological Interview (MINI) (Sheehan et al., 1998) to screen for psychopathology. Each participant was then fitted with an actigraphic sleep monitor wristwatch (Actiwatch Spectrum, Philips Respironics, OR, USA) and shown how to log onto a secure web-based sleep diary to complete daily questions about sleep and activity. Participants were instructed to wear the actigraph watch continuously for the duration of the study and return to the lab for a baseline neurocognitive assessment and MRI scan in one week.

2.2.2. Visit 2: Baseline neurocognitive assessment/MRI scan

After one week of at-home baseline actigraphic sleep assessment, participants returned for a baseline neurocognitive and neuroimaging assessment. Participants arrived at the lab at 8:00 a.m. to complete pre-scan procedures, including a pregnancy test for females and brief practice tasks for the functional portion of the scan. Beginning at 9:00 a.m., participants underwent a 60-min neuroimaging scan that included standard structural MRI (MPRAGE), resting-state functional MRI, and diffusion tensor imaging (DTI). After leaving the scanner at 10:00 a.m., participants completed a half-hour neurocognitive assessment with the Repeatable Battery of Neuropsychological Status (RBANS). Between 10:30–11:00 a.m., polysomnographic electrodes were applied, and the participant underwent the first of three trials of the Multiple Sleep Latency Test (MSLT) at 11:50 a.m. After the MSLT, a break for lunch occurred, followed by administration of a measure of balance and stance stability at 1:15 p.m. A second MSLT occurred at 1:50 p.m. Multiple sleep and symptom questionnaires were administered, followed by the Tower of London at 3:15 p.m., and a third MSLT at 3:50 p.m. After testing, electrodes were removed and the participant was provided with a light therapy device with a full demonstration on its use, as well as a printed instruction brochure that provided detailed information about the use of the device.

2.2.3. 6-week light therapy

Based on a pre-established computer-generated randomization scheme, participants were provided either a BLUE or AMBER light device (described in greater detail below) in a double-blind manner (i.e., participants were not informed that there were different colours of lights and all study staff with direct participant contact were blind to the colour of light device assigned to each participant). Participants were instructed to activate the light device every morning within two hours of awakening, but no later than 11:00 a.m., and use the device continuously for 30 min. When using the device, participants were instructed to place the lightbox at approximately arm's length (20–30 in. distance from the face) at a slight angle (20–40°), so that the light would bathe both sides of the face, and were encouraged to avoid looking directly at the diodes to avoid visual discomfort. The device was programmed to turn off automatically after 30 min of continuous use. Additionally, participants were instructed to log onto a secure website to complete a sleep and light use diary each morning after the completion of light exposure.

2.2.4. Visit 3: Post-treatment neurocognitive assessment/MRI scan

Upon completion of the 6-weeks of daily morning light treatment, participants returned to the lab for a final assessment session, which was virtually identical to the baseline session (Visit 2). At the end of the day, participants returned all equipment and were released from the study.

2.3. Assessment measures

The following assessment measures and devices were used:

2.3.1. Personality and psychodiagnostic assessment

At Visit 1, a trained technician administered the Mini-International Neuropsychiatric Interview (M.I.N.I.), a psychometrically validated scale for assessing psychopathology (Sheehan et al., 1998), and the VA National Traumatic Brain Injury Neurobehavioral Symptom Inventory (NSI) (King et al., 2012). At Visit 2, participants completed several self-report assessment scales including the Beck Depression Inventory (BDI-II) (Beck et al., 1996), Rivermead Postconcussion Symptom Questionaire (RPCSQ) and basic questionnaires regarding sleep history, injury history, caffeine use, and demographics.

2.3.2. Actigraphy

Participants wore an Actiwatch Spectrum (Philips Respironics) wristwatch actigraph to monitor activity and sleep. The device collected wrist activity movement counts and accumulated light exposure every 60 s throughout the duration of the study. After each participant's study run, the activity data were downloaded from the watch.

2.3.3. Sleepiness and subjective sleep need assessment

At each visit, participants completed the Epworth Sleepiness Scale (ESS)(Johns, 1991), a measure of typical daytime sleepiness. Additionally, at seven times during each visit day (8:55 a.m., 10:05 a.m., 11:40 a.m., 1:05 p.m., 1:35 p.m., 2:35 p.m., 3:35 p.m.), participants completed a rapid single-item 7-point Likert assessment of immediate sleepiness with the Stanford Sleepiness Scale (SSS)(Herscovitch and Broughton, 1981). Additionally, as an indicator of perceived sleep need, we also asked participants to indicate “how many hours do you need to sleep to feel your best.”

2.3.4. MSLT

Following the MRI procedure, each participant underwent a polysomnography (PSG) hook-up following standard procedures using the 10–20 system. A total of 14 leads were connected (i.e., A1, A2, O1, O2, Cz, C3, C4, F3, F4, LEOG, REOG, P3, Pz, P4). At three times during the assessment session (i.e., 11:50 a.m., 1:50 p.m., 3:50 p.m.), participants were escorted to a private, infrared video-monitored, sleep chamber to complete the multiple sleep latency test (MSLT). The participant laid supine on a bed and was connected to a Nihon Kohden Polysmith system (software version 11.0), with an amplifier (JE-912AK) and

remote headbox (JE-915A). After standard biocalibration, the participant was instructed to lie quietly and try to relax. The lights were then turned off. PSG recording continued for 20 min and was monitored continuously by a trained technician in real time. The procedure was terminated after 20 min or was ended early if there were three consecutive 30-s epochs of sleep stage N1 or one continuous epoch of any other sleep stage. Each recording was then independently scored by a trained and certified polysomnographic technician to determine the number of minutes of wakefulness before entering into stage N1 or deeper sleep. A score of 20 indicated no sleep was measured.

2.3.5. Psychomotor vigilance test (PVT)

At three times during the course of each assessment session (11:30 a.m., 1:25 p.m., 3:25 p.m.), participants completed a 10-min assessment of attention and vigilance with the psychomotor vigilance test (PVT) (Dinges and Powell, 1985) on a desktop computer. During the task, participants were required to monitor a black screen and press a response key as quickly as possible whenever a target stimulus appeared in the center of the screen. Response time feedback was provided for each response. Each stimulus was presented in a pseudo-random fashion with an inter-stimulus interval that ranged randomly without replacement from 2 to 10 s.

2.3.6. Neurocognitive assessment

From approximately 10:05–10:35 a.m., participants completed the RBANS, a brief battery of well-normed neuropsychological tests that is commonly used for assessing individuals with traumatic brain injury. The test provides several index scores, including: Immediate Memory, Visuospatial/Constructional, Language, Attention, Delayed Memory, and Total Score. Two alternate forms were counterbalanced across the two groups for each administration. Additionally, at approximately 3:15 p.m., participants completed a 10-trial computerized version of the TOL as a measure of executive functioning (i.e., planning and sequencing ability) (Colorado Assessment Tests, http://www.catstests.com). On each trial, the participant began with a starting "tower" that consisted of three "pegs" of differing lengths, each with an arrangement of three different coloured "beads" in various configurations upon the pegs. To solve the puzzle, the examinee must rearrange the beads to match a pre-specified goal pattern as quickly and in as few moves as possible. Dependent variables from this task included the number of moves required to match the goal arrangement, the average total move time, and an index of throughput that accounted for both speed and accuracy (i.e., [(proportion of correct moves)/(average total move time in seconds)] x 0.60).

2.3.7. Light exposure devices

At the conclusion of Visit 2, participants were provided with either a BLUE or AMBER a light therapy device to be used each morning. The devices were manufactured by Philips Electronics (Stamford, CT). All units were identical in design, with the exception of the colour wavelength of the LEDs. Each device consisted of a 13.5 × 14 cm plastic encased table-mounted device with a 10 × 6 array of light emitting diodes (LEDs). Each LED was encased in a 1 × 1 cm cubical projection element covered by a translucent plastic window. For the active BLUE condition, participants were provided with a commercially available Philips goLITE BLU® Energy Light device (Model HF3321/60). The goLITE BLU Energy Light has a narrow bandwidth (peaking at λ = 469 nm, at 214 Lux, and single panel irradiance (mW/cm^2) = 0.11 at 80 cm). The AMBER placebo devices were provided on loan by the manufacturer. The AMBER devices were essentially identical in design to the goLITE BLU devices, with the exception that they were fitted with amber LEDs (peaking at λ = 578 nm, at 188 Lux, and panel irradiance (mW/cm^2) = 0.04 at 80 cm). Participants were instructed to use the device on its highest setting, and the device was set to deactivate after 30 min of continuous use.

2.4. Neuroimaging methods

Data were collected at baseline and post-treatment using a 3.0 T magnetic resonance imaging scanner (Siemens Tim Trio, Erlangen, Germany) using a 32-channel head coil. All scans occurred between 9:00–10:00 a.m.

2.4.1. Structural neuroimaging

Volumetric data were collected using a T1 weighted 3D magnetization-prepared rapid acquisition gradient echo (MPRAGE) sequence (TR/TE/flip angle = 2.1 s, 2.3 ms, 12°) that consisted of 176 sagittal slices (256 × 256 matrix) with a slice thickness of 1 mm and a voxel size of 1 × 1 × 1 mm^3. T1 weighted structural images were preprocessed using the Computational Anatomy Toolbox (CAT12) (http://www.neuro.uni-jena.de/cat/) in SPM12 (http://www.fil.ion.ucl.ac.uk/spm/software/spm12/). Images were realigned to the anterior-posterior commissure axis and then segmented using the longitudinal pipeline into gray matter, white matter, and cerebrospinal fluid using VBM12, a fully automated algorithm in SPM12. Segmented images were used to create a custom DARTEL template and then the images were normalized to Montreal Neurological Institute (MNI) space. Smoothing of normalized images was performed with a 10 mm full width at half maximum (FWHM) isotropic Gaussian kernel.

2.4.2. Functional neuroimaging

Resting-state functional MRI images were acquired for 6 min using a gradient echo T2*-weighted sequence (TR/TE/flip angle = 2 s/30 ms/90°) and a 224 mm FOV. The resting functional images were collected in the same plane with 34 coronal slices and a voxel size of 3.5 × 3.5 × 3.5 mm^3, in an interleaved excitation order, with foot-to-head phase encoding. At the beginning of each scan, four images were acquired and discarded to allow for T1-equilibrium effects. Head movement was restricted using expandable foam cushions, and subjects were asked to remain awake with eyes open while lying still during the scans. Participants were simply instructed to allow their mind to wander during the scan. Resting-state fMRI data were preprocessed in SPM12 (http://www.fil.ion.ucl.ac.uk/spm/software/spm12/). Functional images were slice-time corrected, co-registered to their anatomical images, realigned and resliced to 2 × 2 × 2 mm^3 isotropic voxels, unwarped to correct for field inhomogeneity, normalized to the standard three-dimensional space of the Montreal Neurological Institute (MNI), and spatially smoothed using a 6 mm isotropic Gaussian kernel. Outliers from motion and global signal intensity were identified using the *ART* toolbox https://www.nitrc.org/projects/artifact_detect/. Images with movement from a preceding image exceeding 0.5 mm or a global mean intensity > 3 standard deviations were regressed out of the first level general linear models.

2.4.3. Diffusion tensor imaging (DTI)

DTI scans were acquired using a Siemens Tim Trio 3 T scanner (Erlangen, Germany) at McLean Hospital Imaging Center. Diffusion-weighted imaging (DWI) data were acquired along 72 directions with a b-value of 1000 s/mm^2 and following parameters: voxel size = 1.75 × 1.75 × 3.5 mm^3, TR = 6340 ms, TE = 99 ms, flip angle = 90° and 40 axial slices with thickness = 3.5 mm, encompassing the whole brain. A set of 8 images with no diffusion weighting (b0 images) was also acquired. Using dcm2nii toolbox (part of MRIcron (Rorden et al., 2007)), we converted DWI data from DICOM into NIFTI format. A b-value and b-vector file was generated during this step. The raw data were imported into the DSI Studio (http://dsi-studio.labsolver.org) and converted into SRC format. Each SRC file underwent standard eddy current and subject movement correction, followed by a thorough examination using quality control (QC) procedure to ensure the quality and integrity of data. Neighboring DWI correlation (NDC) values for the current data set were > 0.95. No outlier in NDC values (> 3 median absolute deviation) was identified.

2.5. Data analysis

Data analysis followed a sequential process. First sleep and performance measures were compared between pre- and post-treatment. Second, we compared gray matter volume (GMV) in the brain between pre- and post-treatment using voxel-based morphometry (VBM). As discussed in detail below, two separate clusters within the left and right thalamus demonstrated significant increases in volume following treatment with BLUE light. Third, the resulting significant GMV clusters were used as seed regions of interest (ROIs) in a subsequent resting state functional connectivity (rsFC) analysis. Significant functional connectivity values between the seed ROIs and associated cortical clusters (ROIs) were extracted for further analysis. Fourth, the functional connectivity data were also analyzed using Granger causality (GC) analysis to determine the directional nature of the connectivity patterns. Areas which were not found to be structurally connected were not analyzed using GC. Lastly, the seed and target ROIs resulting from the rsFC analysis were implemented as endpoint regions in a fiber tractography analysis using the diffusion tensor imaging scan data. Once fiber tracts were defined for each individual, standard DTI metrics of fiber pathway integrity were extracted and compared between pre-and post-treatment for each light condition. The resulting metrics from each region were extracted for further analysis with relevant behavioral outcome metrics.

2.5.1. Actigraphic sleep analysis

Actigraphic data were downloaded and then processed and scored in Actiware® 6 (Philips Respironics) according to standardized procedures. For the present analysis, we averaged the minutes of sleep obtained for each overnight sleep opportunity for the first six nights of the baseline week (i.e., between Visit 1 and 2) and the final six nights preceding the post-treatment visit (Visit 3). For each participant, sleep onset time, wake time, sleep duration, sleep efficiency, and wake after sleep onset (WASO) was calculated. A 2 between (light colour: blue vs amber) x 2 within (time: baseline vs post-treatment) mixed analysis of variance (ANOVA) was conducted on each of these variables separately. For all behavioral analyses, we controlled for a set of variables likely to affect sleep, including concussion severity (RPCSQ and occurrence of loss of consciousness (LOC) from the most recent concussion), depression (BDI), and participant age. As appropriate, for select sleep measures, change metrics were also examined as dichotomous outcome variables (i.e., improvement vs. no-improvement) to allow determination of odds ratios (OR).

2.5.2. Cognitive/behavioral performance analysis

To assess the effects of light treatment group on cognitive and behavioral measures, data from self-report questionnaires (e.g., ESS) and cognitive metrics (e.g., TOL) were computed as a change from baseline. These change scores were then compared using one-way ANCOVA, controlling for RPCSQ, LOC, BDI, and age. As appropriate, for select behavioral measures, change metrics were also examined as dichotomous outcome variables (i.e., improvement vs. no-improvement) to allow determination of odds ratios (OR).

2.5.3. GMV statistical analysis

Statistical analyses were conducted in several stages. First, processed GMV data from CAT12 were analyzed in SPM12. A 2 between (blue vs. amber) x 2 within (baseline vs. post-treatment) mixed analysis of variance (ANOVA) was conducted within SPM12 using the flexible factorial option, controlling for age, intracranial volume, and the number of days the light device was used (according to online sleep logs). Maps were cluster corrected for family-wise error (FWE, $p < .05$) at the whole brain level. Resulting clusters were then compared from pre-to post-treatment using paired *t*-tests in SPM12 for the BLUE light group, with age, intracranial volume, and the number of total days in the study during which participants reported using the light device entered as nuisance covariates. To increase precision, separate search territories were placed for the left and right thalamus using the automated anatomic labeling atlas (AAL; (Tzourio-Mazoyer et al., 2002)). We used a cluster-extent based thresholding, following the recommended approach suggested by Woo, Krishnan, and Wager (Woo et al., 2014), applying a primary significance threshold of $p < .001$, uncorrected, as the default lower limit. Based on this primary height threshold, SPM12 provided the critical cluster size for cluster-extent correction with family-wise error (FWE) maintained at $p < .05$ for the search territory. Between group *t*-tests were conducted for the BLUE group and resulting significant clusters were used a regions of interest (ROIs) that were then compared for the AMBER group to constrain for multiple comparisons. Using the Region Extraction Tool (REX), the mean GMV estimates were extracted for each cluster for the BLUE and AMBER groups separately and exported to IBM SPSS Statistics 25 for further analyses.

We were interested in the associations between the change metrics for each neuroimaging parameter and several cognitive/behavioral outcome variables. Here, the volumetric change values for each cluster were extracted for each individual for correlation with cognitive/behavioral measures of interest. A hierarchical multiple regression procedure was employed, including covariates for age, intracranial volume, and the number of days the light was used (as determined from online sleep logs) in the first block of the analysis, followed by the specific change values for GMV in the second block. After controlling for covariates, the partial correlation coefficient calculated between GMV change and the cognitive/behavioral metrics.

2.5.4. Functional connectivity analysis

A single subject was removed from each group from subsequent fMRI analyses, as > 20% of their scans were identified as outliers. An independent samples *t*-test indicated no significant difference between groups in the number of outliers identified and incorporated into subsequent first level models at baseline ($p = .09$) and post-treatment ($p = .54$).

Here, we used the two GMV clusters identified in the previous analysis (i.e., left pulvinar (LPul) and right pulvinar (RPul)) as seed regions for resting state functional connectivity (rsFC) analyses. Functional connectivity analyses were performed with a seed-to-voxel driven approach within the CONN toolbox V17.f (Whitfield-Gabrieli and Nieto-Castanon, 2012). Preprocessed structural and resting state data had physiological and other noise sources identified as nuisance covariates using a component-based noise correction method (CompCor). The first acquisition image, images identified as outliers, nuisance covariates, as well as white matter and cerebrospinal fluid masks, were regressed out of the first level general linear models. The BOLD time series was then band pass filtered at 0.01–0.1 Hz. Individual subject seed-to-voxel whole-brain connectivity maps were created for the LPul and RPul seeds with the mean time series from each seed used as a predictor in a multiple regression General Linear Model (GLM). The resulting individual bivariate correlation coefficients were Fisher transformed into *Z*-scores for subsequent second level analyses.

2.5.4.1. Seed-to-voxel analysis. Two analyses were performed at the second level to create statistical parametric maps (SPMs) representing associated changes in functional connectivity for each seed region. Repeated measures two-way ANCOVAs were used to investigate the main effect on functional connectivity associated with BLT, with mean-centered age and mean-centered days light used as covariates within the models. SPMs for each seed were defined with a cluster-forming threshold (voxel-level uncorrected $P < .001$) and a cluster-level extent threshold (Family Wise Error (FWE) corrected $P < .05$), using a positive contrast, to identify clusters of voxels associated with significant increases in connectivity to the seed region. No clusters were identified using the RPul seed, and three clusters were identified using the LPul seed. A mask was created for each cluster identified containing voxels that correlated with the LPul seed, in order to further

investigate Regions of Interest (ROIs) that contained voxels associated with significant change for the treatment group.

2.5.4.2. Seed-to-ROI analysis. To determine the extent of connectivity change observed for either treatment group, the BOLD time-series was extracted from each cluster identified in the seed-to-voxel analyses. Seed-to-ROI within group connectivity analyses were performed using paired *t*-tests with the identified ROIs (i.e. Left Parietal Cortex: LParC, Left Agranular Frontal Area: LAFA, and the Right Parietal Cortex: RParC), and the LPul seed. Mean-centered age and mean-centered days light used were included in the models as covariates and results were corrected for multiple comparisons ($p < .05$, seed-level FDR-correction).

The functional connectivity values for each connection were extracted for each individual for further correlation with cognitive/behavioral measures of interest. We applied hierarchical multiple regression procedures, including covariates for age and the number of days the light was used (as determined from online sleep logs) in the first block of the analysis, followed by the specific functional connectivity parameter of interest in the second block. After controlling for covariates, the partial correlation was determined for the parameters of interest.

2.6. Directed functional connectivity (DFC) analysis: Granger causality (GC)

Raw time-series data were band pass filtered using the Butterworth filter design using higher cutoff frequency of 0.0028 Hz (f_1) and a lower cutoff frequency of 0.1 Hz (f_2). Higher cutoff frequency was determined from time-series length ($n = 180$ time-points) and repetition time (TR = 2 s) as following:

$$f_1 = \frac{1}{n * TR} = 0.0028\text{Hz}$$

The lower cutoff frequency of 0.1 Hz was selected because low frequency (< 0.1 Hz) BOLD fluctuations often show strong correlations at rest (Cordes et al., 2001). The ensemble means from the time-series for each node were removed to make the zero-mean process for GC analysis. Moreover, these steps helped to remove slow trends and physiological noise associated with respiratory and cardiac activities.

A spectral interdependency method (Dhamala, 2013) was used to estimate the DFC between ROIs by quantifying the inter-relationships between their corresponding oscillatory mechanisms as a function of frequency (f) of oscillations. Directional influences between two regions, say a and b, are estimated from a spectral density matrix (S). Matrix S is constructed parametrically from the time-series of systems a and b using autoregressive (AR) modeling as following:

$$GC_{a\to b} = \ln \frac{S_{bb}(f)}{\widetilde{H}_{aa}(f)\sum_{aa}\widetilde{H}^{*}_{aa}(f)}$$

$$GC_{b\to a} = \ln \frac{S_{aa}(f)}{\widetilde{H}_{bb}(f)\sum_{bb}\widetilde{H}^{*}_{bb}(f)}$$

Here, $\widetilde{H}_{aa} = H_{aa} + \frac{\sum_{ab}}{\sum_{aa}}H_{ab}$ and $\widetilde{H}_{bb} = H_{bb} + \frac{\sum_{ab}}{\sum_{bb}}H_{ba}$ represent new transfer function matrices for a and b respectively in terms of noise covariance matrix, Σ and transfer function matrix *H*. Here, * denotes matrix adjoint. Mathematical details of these estimations are documented previously (Dhamala, 2013).

GC measures can be computed by either parametric or non-parametric methods (Dhamala et al., 2008a; Dhamala et al., 2008b). In this study, we used the parametric approach. The optimal model order for parametric approach was calculated by comparing power spectra from the parametric and non-parametric approaches (Dhamala et al., 2008a). Different model orders from 1 to 10 were tested, and the model order, which yielded the lowest power difference, was selected. The threshold level for statistically significant directed functional connection was estimated from surrogated data by using permutation test ($n = 1000$) and a gamma function under a null hypothesis of no interdependence at the significance level of $p < 10^{-4}$ (Blair and Karniski, 1993; Brovelli et al., 2004) ($p = 10^{-4}/16$, corrected for multiple comparisons). Previously, the GC technique has been shown to have consistent results with the dynamic causal modeling technique, in terms of directional connectivity from resting-state fMRI data (Bajaj et al., 2016).

For the present analyses, the range of GC metrics was extracted for each individual and correlated with cognitive/behavioral measures of interest. Using hierarchical multiple regression procedures, covariates including age, intracranial volume, and the number of days the light was used were entered at a first block, followed by the specific GC range parameter of interest at the second block, and the partial correlation was determined for the parameters of interest.

2.7. Anatomical connectivity analysis: DTI

Diffusion MRI connectometry (Yeh et al., 2016) was performed to compare longitudinal pair-wise scans between pre and post-treatment conditions for both amber-light treatment (ALT) and blue-light treatment (BLT) groups. The connectometry approach, which is implemented in DSI Studio, uses a permutation test to perform the longitudinal pairwise comparison between white-matter pathways. Tracts, which showed significant longitudinal differences along axonal fiber directions, were identified using a deterministic tractography algorithm (Yeh et al., 2013). Group averages of local connectome were quantified in terms of their differences in density and diffusivity measurements of water diffusion, *including* fractional anisotropy (FA) as well as isotropic (ISO) diffusion. Here, FA is one of the most common *diffusivity* measures, which is defined for each voxel and represents how fast water diffuses, whereas ISO is a *density* measure and represents how much water diffuses in an isotropic fashion. Both FA and ISO components were estimated using the Q-space diffeormophic reconstruction (QSDR) (Yeh and Tseng, 2011) approach implemented in DSI Studio. QSDR is a model-free approach, which calculates the distribution of water diffusion using a high-resolution standard brain atlas constructed from 90-diffusion spectrum imaging datasets in the ICBM-152 space. Automated registration to standard template space was used for each subject. All the regions of interest (ROIs) were transformed into MNI space in order to perform diffusion MRI connectometry in QSDR-space. A seed-count of 5000 sub-voxels for each region (LPul, LParC and LAFA) was used for connectometry analysis. All the ROIs were dilated to 3 mm to extend to white matter. Tracts with differences in FA and ISO diffusion were identified for all the connections, which showed significant involvement in functional connectivity analysis i.e., between LPul and LParC and between LPul and LAFA. To limit the tracts between LPul and LAFA, LPul was used as a seed region as well as an end region and LAFA was used as an end region. A lower T-value threshold of 0.5 was used to identify tracts which were more sensitive to light treatment. Track pruning was conducted using 10 iterations, and tract length threshold was 30 voxels. A total of 10,000 permutations and false discovery rate (FDR) of 0.05 were used to obtain the null distribution of the tract length. Subject-wise differences for the tracts that showed differences (at FDR between 0 and 0.2) in either FA or ISO diffusion measures were extracted for further correlation analysis with behavioral parameters. Using hierarchical multiple regression procedures, covariates including age, intracranial volume, and the number of days the light was used (as determined from online sleep logs) were entered at a first block, followed by the specific ISO diffusion parameter of interest at the second block, and the partial correlation was determined for the parameters of interest.

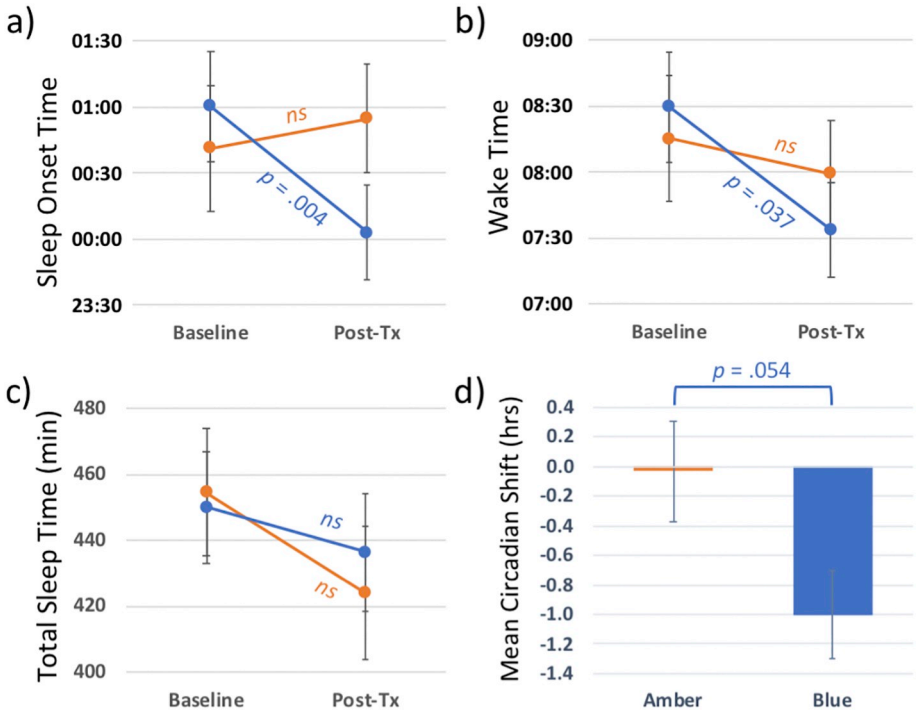

Fig. 3. Effects of light treatment on actigraphic sleep measures. (a) Blue light shifted sleep onset time by 57.5 min earlier by the end of treatment, versus no change for the amber group. (b) Blue light shifted wake time by 55.9 min earlier by the end of treatment, but there was no difference for amber light. (c) There was no significant effect of light condition for change in total sleep time (TST) from pre- to post-treatment. (d) A comparison of the midpoint of sleep onset and wake time for each light group showed that blue light was associated with a non-significant trend toward a circadian phase advancement in the sleep period of 60.1 min by the end of treatment. Error bars represent 1 SE. (For interpretation of the references to colour in this figure legend, the reader is referred to the web version of this article.)

3. Results

3.1. Baseline metrics

As evident in Table 1, light condition groups were similar on key variables at baseline, including sex, age, years of education, number of previous concussions, months since injury, concussion severity, depression, functional outcomes of sleep, chronotype, and days of compliance with light treatment (determined from daily time-stamped website diary completion). Half of participants (n = 16) reported only one concussion, while half reported more than one lifetime concussion (range 1 to 7 total). Of those reporting more than one concussion, the modal response (i.e., endorsed by 5 participants) was 2 head injuries.

3.2. Actigraphic sleep

BLUE light produced a significant phase advance in sleep onset and offset times relative to AMBER light. After accounting for covariates (baseline concussion symptoms, loss of consciousness (LOC) from the most recent concussion, depression (BDI), age), there was a significant light-condition x time interaction, $F(1, 21) = 6.16$, $p = .022$ (Fig. 3a). Over the course of treatment, planned comparisons showed that participants in the BLUE condition were phase advanced in sleep onset times, generally falling asleep 57.5 min earlier in the final week of the study compared to baseline ($p = .004$), while those in the AMBER condition fell asleep 13.8 min later compared to baseline ($p = .508$). Overall, 80% of participants in the BLUE condition showed some evidence of earlier sleep onset, while 58.3% of those in the AMBER group did ($\chi^2 = 1.50$, $p = .221$). After accounting for covariates (described above), the odds ratio (OR) for showing any phase advancement with BLUE light compared to AMBER was 13.04 (95% CI: 0.84 to 202.52; $p = .066$. Further, planned comparisons showed that participants in the BLUE condition were awakening 55.9 min earlier by the final week of treatment compared to baseline ($p = .037$), whereas the AMBER condition was awakening only 16.1 min earlier after treatment ($p = .576$; see Fig. 3b). Overall, 66.7% of participants in the BLUE condition showed some evidence of earlier wake times, while 50% of those in the AMBER group did ($\chi^2 = 0.77$, $p = .38$). After accounting for covariates (described above), the odds ratio (OR) for showing any phase advancement with BLUE light compared to AMBER was 3.68 (95% CI: 0.55 to 24.74; $p = .18$. There were no significant changes in mean total sleep time (TST) per night between pre- and post-treatment assessments, regardless of light-condition (all p-values > .05; see Fig. 3c). There was a nonsignificant trending difference between light-condition groups in the extent of circadian phase shift (CPS; i.e., taking the midpoint between sleep onset and offset for each participant) from baseline, $F(1, 21) = 4.18$, $p = .054$ (see Fig. 3d), such that those in the BLUE light condition showed an average circadian phase advance in the midpoint of the sleep period of 60.1 min, whereas those in the AMBER light condition shifted earlier by only 1.9 min on average. Overall, while 73.3% of participants who received BLUE light showed at least some evidence of phase advancement, 58.3% of those in the AMBER group also showed at least some phase advancement ($\chi^2 = 0.675$, $p = .411$). After accounting for covariates (described above), the odds ratio (OR) for showing any phase advancement with BLUE light compared to AMBER was 7.34 (95% CI: 0.59 to 90.71; $p = .12$.

3.3. Sleepiness and subjective sleep need

Relative to placebo, the BLUE light intervention led to reduced typical daytime sleepiness $F(1,26) = 5.49$, $p = .027$ (see Fig. 4a). Moreover, we found that 87.5% of the participants in the BLUE light condition showed reduced sleepiness scores from pre- to post-treatment, whereas only 37.5% of those in the AMBER placebo condition showed any measurable reduction in sleepiness over the same time frame (($\chi^2 = 8.53$, $p = .003$; see Fig. 4b). After controlling for covariates (described above), the odds ratio (OR) for showing any improvement in daytime sleepiness was 25.63 (95% CI: 2.76 to 237.84; $p = .004$; Nagelkerke $R^2 = 0.446$). We also found that the number of hours necessary to subjectively "feel best" was reduced for the BLUE light condition ($M = -1.51$, $SE = 0.47$) relative to AMBER ($M = 0.043$, SE = 0.47), $F(1,26) = 4.99$, $p = .034$ (see Fig. 4c).

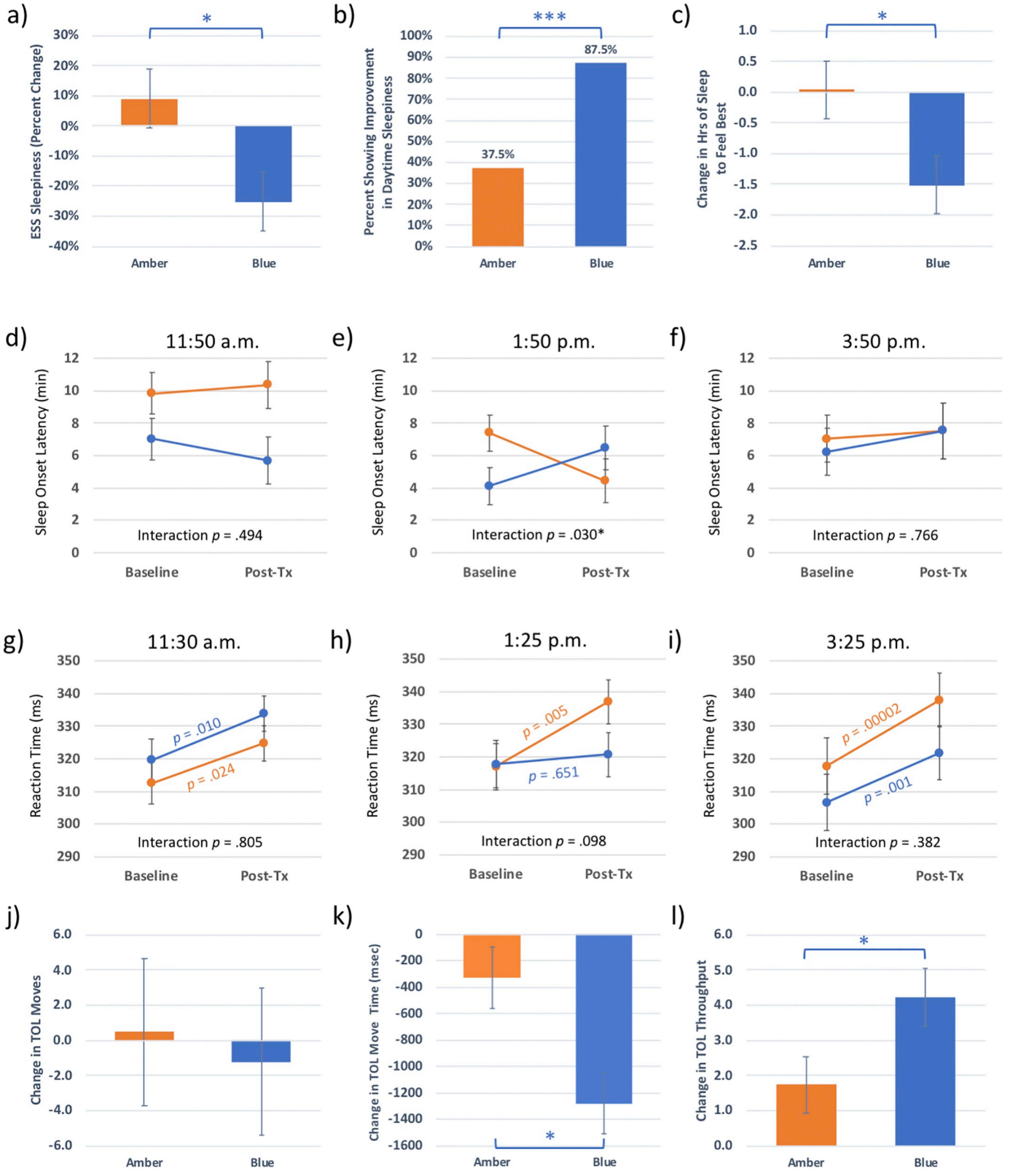

(caption on next page)

Fig. 4. Effects of light treatment on behavioral variables. (a) Blue light led to a significant reduction in daytime sleepiness scores on the Epworth Sleepiness Scale (ESS), with (b) a significantly greater percentage of blue light participants showing some improvement in daytime sleepiness relative to amber participants. (c) Blue light was associated with a significant reduction in the number of nightly hours of sleep that participants reported needing to feel their best, relative to the amber group. (d-f) Sleep onset latency on the multiple sleep latency test (MSLT) was unaffected by light condition in the late morning (11:50 a.m.) or late afternoon (3:50 p.m.), but showed a significant interaction for the early afternoon "post-lunch dip" period. Similarly, (g-i) psychomotor vigilance test reaction time did not differ between groups during the late morning (11:30 a.m.) or late afternoon (3:25 p.m.), but was affected by blue light only in the early afternoon. Although there was (j) no effect of light condition on the total number of moves from the Tower of London (TOL) test, (k) blue light was associated with a significant improvement in average bead movement times relative to amber light, and (l) when speed and accuracy were combined as a metric of "throughput", blue light was associated with significantly more correct moves per minute than the amber placebo group. (*$p < .05$), **$p < .01$, ***$p < .005$). (For interpretation of the references to colour in this figure legend, the reader is referred to the web version of this article.)

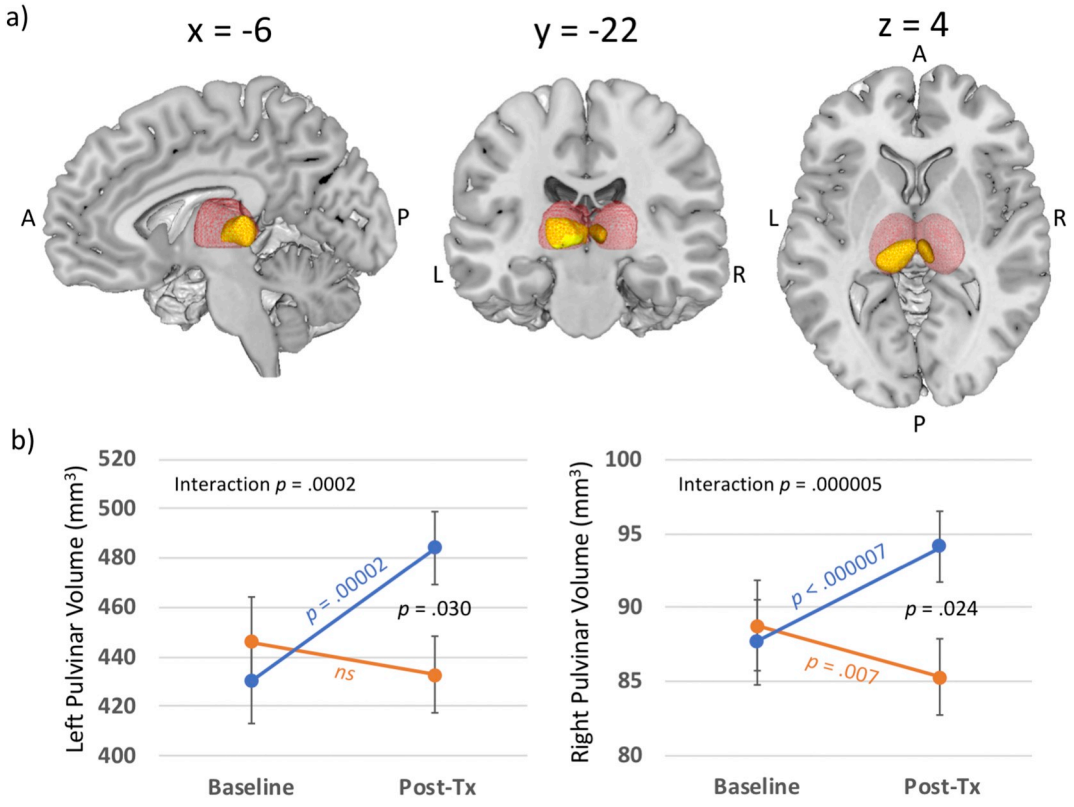

Fig. 5. Voxel-based morphometry results for blue versus amber light treatment. Results of a whole brain voxel-based morphometry (VBM) analysis comparing baseline and post-treatment changes for those receiving the blue light condition. (a) The figure shows the sagittal (left) coronal (middle) and axial (right) orientations. This analysis showed significant increases in gray matter volume (GMV) within the left (567 voxels; MNI: x = −3, y = −22, z = 3) and right (119 voxels; MNI: x = 3, y = −22, z = 3) posterior thalamic volume for those receiving the BLUE light intervention ($p_{FWE} < 0.05$). (b) Extracted volumes from each of these clusters are plotted in the figures for visualization for the left and the right thalamic regions for the BLUE and AMBER groups separately. The location of the left and right thalami are represented by the red wire mesh areas of the figure. It is clear that BLUE light was associated with significant increases in the volume of both the left and right posterior regions, but this was not evident for the same regions in the AMBER group. (For interpretation of the references to colour in this figure legend, the reader is referred to the web version of this article.)

3.4. MSLT

As an objective measure of daytime sleepiness/alertness, participants completed a modified version of the MSLT over three time points at baseline and post-treatment. Notably, it was only the second MSLT, occurring in the early afternoon (1:50 p.m.) proximal the "post-lunch dip" (Monk, 2005), that showed a significant light-condition x time interaction, $F(1, 26) = 5.26$, $p = .030$ (see Fig. 4d–f), suggesting that from pre- to post-treatment, participants in the BLUE light condition showed increased latency to fall asleep during the mid-day (i.e., were more alert). There were no significant light-condition x time interactions for the early morning or late afternoon MSLT sessions.

3.5. Cognitive/behavioral performance

Participants completed multiple cognitive and behavioral tasks at baseline and after 6-weeks of intervention with either the BLUE or AMBER light.

3.5.1. Psychomotor vigilance

At the first psychomotor vigilance test (PVT), which occurred in the late morning (11:30 a.m.), there was no significant light-condition x time interaction, $F(1, 22) = 0.062$, $p = .805$ (see Fig. 4g), with both groups slowing in reaction time (RT) during the post-treatment session relative to baseline, and no group differences. By the second PVT, in the early afternoon (1:25 p.m.), near the "post-lunch dip", there was a non-significant light-condition x time interaction, $F(1, 22) = 2.985$, $p = .098$ (see Fig. 4h), with post-hoc tests indicating that from pre- to post-treatment, participants in the AMBER light condition showed significant slowing of RT ($p < .005$), while those participants in the BLUE light condition sustained RT from pre- to post-treatment. Finally, by late afternoon (3:25 p.m.), the light-condition x time interaction remained non-significant $F(1, 22) = 0.797$, $p = .382$ (see Fig. 4i).

3.5.2. Neuropsychological performance

Contrary to predictions, light condition had no significant effect on mean performances on a brief neurocognitive performance battery (RBANS), which included immediate Memory, Visuospatial/Constructional, Language, Attention, Delayed Memory, and RBANS Total Score.

3.5.3. Executive functioning

On the Tower of London (TOL), a classic executive function planning task, the light condition did not affect the number of moves required to solve the puzzles between pre- and post-treatment, $F(1,26) = 0.08$, $p = .79$ (see Fig. 4j). However, the light-condition did affect the time taken to solve the puzzles, $F(1,26) = 7.45$, $p = .01$ (see Fig. 4k). On average, participants who underwent the BLUE wavelength light condition were 1280 (SE = 234) ms faster in completing each move following treatment, while those in the AMBER placebo condition improved by only 325 (SE = 234) ms per move. When speed and accuracy were combined as a measure of "throughput," there was a significant effect of light condition, $F(1,26) = 4.26$, $p = .049$. As shown in Fig. 4l, participants in the BLUE light condition showed an increase in the number of correct bead placements of 4.23 (SE = 0.83) per minute, whereas those in the AMBER condition increased by only 1.73 (SE = 0.83) per minute after treatment. Overall, most participants showed at least some improvement in TOL performance, regardless of condition, with 93.8% of participants in the BLUE group and 81.3% of participants in the AMBER group showing greater throughput after 6-weeks ($\chi^2 = 1.143$, $p = .285$). After accounting for covariates (described above), the odds ratio (OR) for showing any improvement in throughput with BLUE light compared to AMBER was 6.50 (95% CI: 0.41 to 102.15; $p = .183$.

3.6. Gray matter volume (GMV)

To examine morphometric volume changes in the brain, the anatomical brain images obtained during the MRI scan were analyzed in SPM12 with a 2 between (BLUE vs. AMBER) x 2 within (baseline vs. post-treatment) mixed analysis of covariance (ANCOVA), controlling for age, intracranial volume, and the number of days the light device was used. The ANCOVA yielded a large bilateral cluster (807 voxels, $p_{FWE} < 0.05$; MNI: x = 0, y = −21, z = 3) reflecting a significant light dependent change in volume from pre- to post-treatment. This region was constrained to the pulvinar regions of the left (LPul) and right (RPul) thalamus (Fig. 5a). Given the significant interaction, we examined the effects of each light condition individually. As shown in Fig. 5b, a pre- to post-treatment *t*-test for those receiving the BLUE light condition showed that this effect was driven primarily by an increase in thalamic GMV (bilateral) ($p_{FWE} < 0.05$), but this was not evident for the AMBER light condition.

Multiple regression was used to determine the partial correlations between changes in pulvinar volume and performance metrics. As shown in Fig. 6a–c, after controlling for age, intracranial volume, and the number of days of light device use, greater volume increases in the pulvinar region of the left thalamus were associated with faster bead pickup time, faster total move time on the TOL, and with a slight increase in subjective ratings of sleepiness at post-treatment, measured using the SSS. Right thalamic volume changes were not associated with any measured changes in cognitive/behavioral scores.

3.7. Functional connectivity

Building on the GMV findings above, we used the two previously identified thalamic clusters (i.e., LPul and RPul) as seed regions in a seed-to-voxel and seed-to-ROI resting state functional connectivity (rsFC) analysis. Repeated measures two-way ANCOVAs were used to investigate the main effect of light-condition on rsFC from pre- to post-treatment.

3.7.1. Seed-to-voxel analysis

Relative to the AMBER light condition, individuals in the BLUE light condition showed increased rsFC from pre- to post-treatment between the LPul seed and voxels comprising three separate areas (Fig. 7a), including a region in the left parietal cortex (LParC; $\beta = 0.34$, $p = .001$), the right parietal cortex (RParC; $\beta = 0.31$, $p < .001$), and left agranular frontal area (LAFA; $\beta = 0.34$, $p < .001$). In contrast, the RPul seed region did not show any significant increase in connectivity with other voxel clusters in the brain.

3.7.2. Seed-to-ROI analysis

Within each light-condition, we examined the ROI-to-ROI connectivity. Consistent with the seed-to-voxel analysis, mean rsFC was significantly increased for the BLUE light condition over the course of treatment between the LPul and the three ROIs, including the LParC, $t(25) = 2.38$, $p = .03$, RParC, $t(25) = 2.26$, $p = .03$, and LAFA, $t(25) = 2.33$, $p = .03$). For the AMBER light condition, significant decreases in connectivity over the course of treatment between the LPul and ROIs were found for all three ROIs, including the LParC, $t(25) = -3.58$, $p = .002$, RParC, $t(25) = -3.65$, $p = .001$, and LAFA, $t(25) = -4.16$, $p < .001$ (Fig. 7b).

As shown in Fig. 6d–g, after controlling for standard covariates, increased rsFC between LPul and LParC ROIs from pre- to post-treatment was associated with a significant reduction in daytime sleepiness on the ESS ($r(23) = -0.50$, $p = .011$), increased scores on RBANS Language ($r(23) = 0.418$, $p = .038$), TOL average bead pickup time ($r(23) = -0.439$, $p = .028$), and TOL Average total move time ($r(23) = -0.411$, $p = .041$). Similarly, increased rsFC between the LPul and RParC was also associated with faster bead pickup time on the TOL ($r(23) = -0.425$, $p = .034$; Fig. 6h).

3.8. Granger causality (GC)

To determine if the rsFC connectivity change was "bottom-up" (i.e., increased thalamocortical connectivity) or "top-down" (i.e., increased corticothalamic connectivity), we next employed GC to determine the directional influence between the previously identified areas of interest. The previous analysis revealed that FC was only evident for the left pulvinar connections (i.e., LPul—LParC, LPul—LAFA, and LPul—RParC). However, we did not find structural connectivity between LPul and RParC for any subject/condition; therefore only four connections (C1: LPul to LParC, C2: LParC to LPul, C3: LPul to LAFA, and C4: LAFA to LPul) were further interrogated using GC.

GC-frequency spectra for all four directional connections (C1, C2, C3, and C4) were computed. The estimated threshold level of GC strength used to identify significant connections was 0.0142 at $p < 10^{-4}$ (permutation method; corrected for multiple comparisons). In Fig. 7c–f, it is evident that GC-frequency spectra for all four connections and for all four conditions (AMBER: APre-T (Amber-light pre-treatment), APost-T (Amber-light post-treatment); BLUE: BPre-T (Blue-light pre-treatment) and BPost-T (Blue-light post-treatment)) had peaks at frequency < 0.1 Hz, and showing the connectivity patterns for APost-T (Fig. 7d) and BPost-T (Fig. 7f). Within the AMBER group, we found that the C1 connection exceeded threshold only at baseline (APre-T), but that connection did not exceed the threshold at APost-T (Fig. 7c). By contrast, in the BLUE group, this same connection did not reach the threshold at BPre-T, but exceeded the threshold at BPost-T (Fig. 7e–f). Connection C2 did not exceed the threshold for either BLUE or AMBER conditions (Fig. 7c and e). In addition, two connections (C3 and C4) exceeded the threshold for connectivity at pre- and post-treatment for both the AMBER and BLUE groups, suggesting that these connections were not meaningfully affected by light condition. In sum, the findings suggest that connection C1 (LPul to LParC) was significantly affected by light condition, showing a decrease in directed bottom-up connectivity in the AMBER group and an increase in this bottom-up connectivity within the BLUE group. Other connections

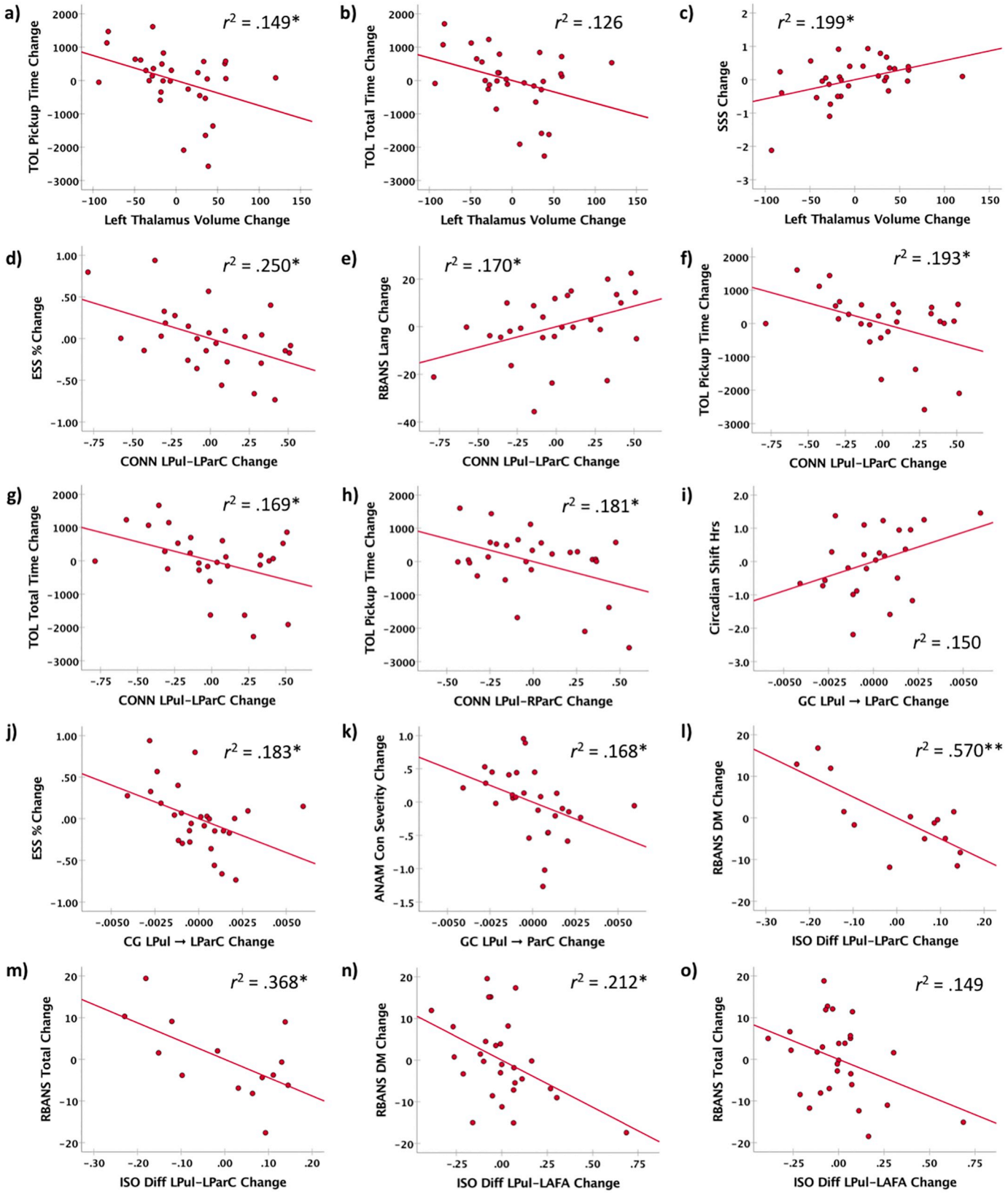

(caption on next page)

Fig. 6. Association of changes in behavioral measures with changes in voxel-based morphometry, directed connectivity strength, and isotropic diffusion (ISO). Greater increases in the volume of the left pulvinar region of the thalamus was associated with (a) faster pickup speed, (b) a trend toward faster total move time on the Tower of London (TOL), and (c) slight increases in subjective sleepiness on the Stanford Sleepiness Scale (SSS). Changes in functional connectivity strength from pre- to post-treatment for the Left Pulvinar (LPul) and Left Parietal Cortex (LParC) were associated with (d) decreases in daytime sleepiness on the Epworth Sleepiness Scale (ESS), (e) improvements in language processing on the Repeatable Battery for Neuropsychological Assessment (RBANS), (f) faster average bead pickup time on the TOL, (g) faster total move time on the TOL. Similarly, increased functional connectivity between the LPul and Right Parietal Cortex (RParC) was associated with (h) faster total move time on the TOL. We found a significant positive association between changes in directed connectivity strength (LPul to LParC) and (i) changes in circadian shifts, and significant negative associations with (j) changes in daytime sleepiness, and (k) scores on the concussion severity scale. We also found a significant negative association between changes in ISO for fibers connecting LPul and LParC and (l) changes in delayed memory scores, as well as (m) total scores on RBANS battery. ISO for fibers connecting LPul and LAFA also showed a significant negative association with (n) changes in delayed memory scores and (o) total scores on RBANS battery.

either remained below the threshold or were essentially unchanged by light condition.

As in the previous analyses, we also examined the cognitive/behavioral correlates associated with changes in causal flow. As shown in Fig. 6i–k, after controlling for age, intracranial volume, and the number of days of light device use, increased causal influence of LPul on LParC from pre- to post-treatment was not significantly associated with change in circadian phase (r (19) = 0.387, p = .083), but was associated with a significant reduction in typical daytime sleepiness on the ESS (r (23) = −0.427, p = .033), and a significant reduction in concussion severity scores on the ANAM (r (23) = −0.409, p = .042).

3.9. Anatomical connectivity

We next examined whether the connectivity changes reported above would be associated with corresponding changes within axonal tracts connecting the identified regions.

We found that there were no tracts with significant differences between pre- and post-treatment for fractional anisotropy (FA) (FDR > 0.05) in either AMBER or BLUE light conditions (Fig. 8a). However, we found tracts connecting LPul and LParC with a significant reduction in isotropic diffusion (ISO) (a measure of white matter disintegrity) following treatment for the BLUE (Fig. 8b) (FDR < 0.05), but not for the AMBER light condition (FDR > 0.05). Furthermore, we found that tracts connecting LPul and LAFA showing reduced ISO diffusion following treatment for the BLUE light condition at a less stringent threshold (FDR = 0.11) (Fig. 8b) and a significant increase in ISO following treatment for AMBER light condition (FDR < 0.05) (Fig. 8c).

We examined the cognitive/behavioral correlates of changes in ISO diffusion within specific white matter tracts discussed above. For the BLUE light condition, subject-wise differences for the tracts connecting LPul and LParC, and LPul and LAFA, were extracted. For the AMBER light condition, subject-wise differences for the tracts connecting LPul and LAFA were extracted. As shown in Fig. 6l–o, only changes in RBANS measures showed significant associations with changes in white matter integrity. Specifically, after controlling for age, intracranial volume, and the number of days the light device was used, decreases in ISO diffusion from pre- to post-treatment for the BLUE light condition were associated with improved visual construction (RBANS VC) performance (r (9) = −0.714, p = .014), improved delayed memory (RBANS DM) performance (r (9) = −0.755, p = .007), and improved total neuropsychological (RBANS Total) performance (r (9) = −0.607, p = .048). For the sample as a whole, decreases in ISO diffusion between LPul and LAFA were associated with improved delayed memory (RBANS DM) performance (r (23) = −0.460, p = .021), and a trend toward greater total neuropsychological (RBANS Total) performance (r (23) = −0.386, p = .057).

4. Discussion

During a 6-week randomized placebo-controlled trial of daily light exposure, we found that 30-min of morning blue-wavelength light was more effective than amber-wavelength placebo light at shifting sleep-wake periods, reducing subjective and objective sleepiness, and improving cognitive performance among participants recovering from mTBI. Moreover, compared to amber light, the blue light intervention was associated with increases in gray matter volume within the posterior thalamus and greater structural and functional thalamocortical connectivity, as well as multiple associations between improvements in cognitive performance and the observed physiological changes. These findings are consistent with the hypothesized role of morning blue-wavelength light in phase advancing the circadian rhythm of sleep and alertness, and the postulated role of sleep in accelerating neural repair processes. Together, these findings point to the ipRGC-SCN-mediated circadian system as a critical contributor to brain repair processes and suggest a potential target mechanism for intervention to facilitate recovery following brain injury.

Our findings are consistent with well-established evidence that blue light exposure affects the timing of sleep-wake cycles through stimulation of the retinohypothalamic system (Geerdink et al., 2016), as we found that the BLUE light condition showed a trend toward phase-advancement of the midpoint of participants' sleep periods by just over one hour by the end of treatment, with no meaningful change observed for the AMBER light condition. Notably, this alteration in sleep timing was not associated with a measurable change in total sleep time based on actigraphy. While light treatment has shown robust effects for shifting sleep timing (Geerdink et al., 2016; Rosa et al., 2018; Tahkamo et al., 2018), prior research demonstrates mixed outcomes in terms of modifying total sleep time (TST) or subjective perception of time spent asleep (Figueiro et al., 2014; Richardson et al., 2018; Saxvig et al., 2014; Wu et al., 2018). It should be borne in mind, however, that our primary measure of TST was based entirely on wrist-actigraphy, which has a satisfactory accuracy level (> 80%) (Marino et al., 2013), but may not be sensitive enough to detect the subtler effects of light treatment on sleep architecture.

Recent work demonstrates that daily morning blue light therapy improves subjective fatigue and daytime sleepiness in patients with TBI (Sinclair et al., 2014). Our results extend these earlier findings, as our BLUE light condition led to a significant decline in subjective daytime sleepiness and a reduction in self-perceived sleep requirement relative to the AMBER placebo condition. Thus, even though BLUE light did not lead to an increase in total sleep time after treatment, participants treated with BLUE light reported a reduced tendency to “doze” off throughout the day, as well as a decrease in the total time asleep necessary to feel their best. Moreover, BLUE light use was also associated with objectively greater daytime alertness, as evidenced by extended latencies to fall asleep during the early afternoon post-lunch dip, compared to the placebo condition, when measured using polysomnography. The blue-wavelength light intervention was also associated with sustained psychomotor vigilance performance in the early afternoon. Thus, the treatment is associated with improvements in both subjective and objective daytime alertness for individuals recovering from mTBI during times when drowsiness is particularly likely to occur.

When directly comparing the groups on neurocognitive performance, we found a clear superiority in blue-wavelength treatment compared to a placebo light treatment on performance during the TOL, a classic test of visual planning and sequencing ability. Relative to AMBER light, daily exposure to BLUE light in the morning was

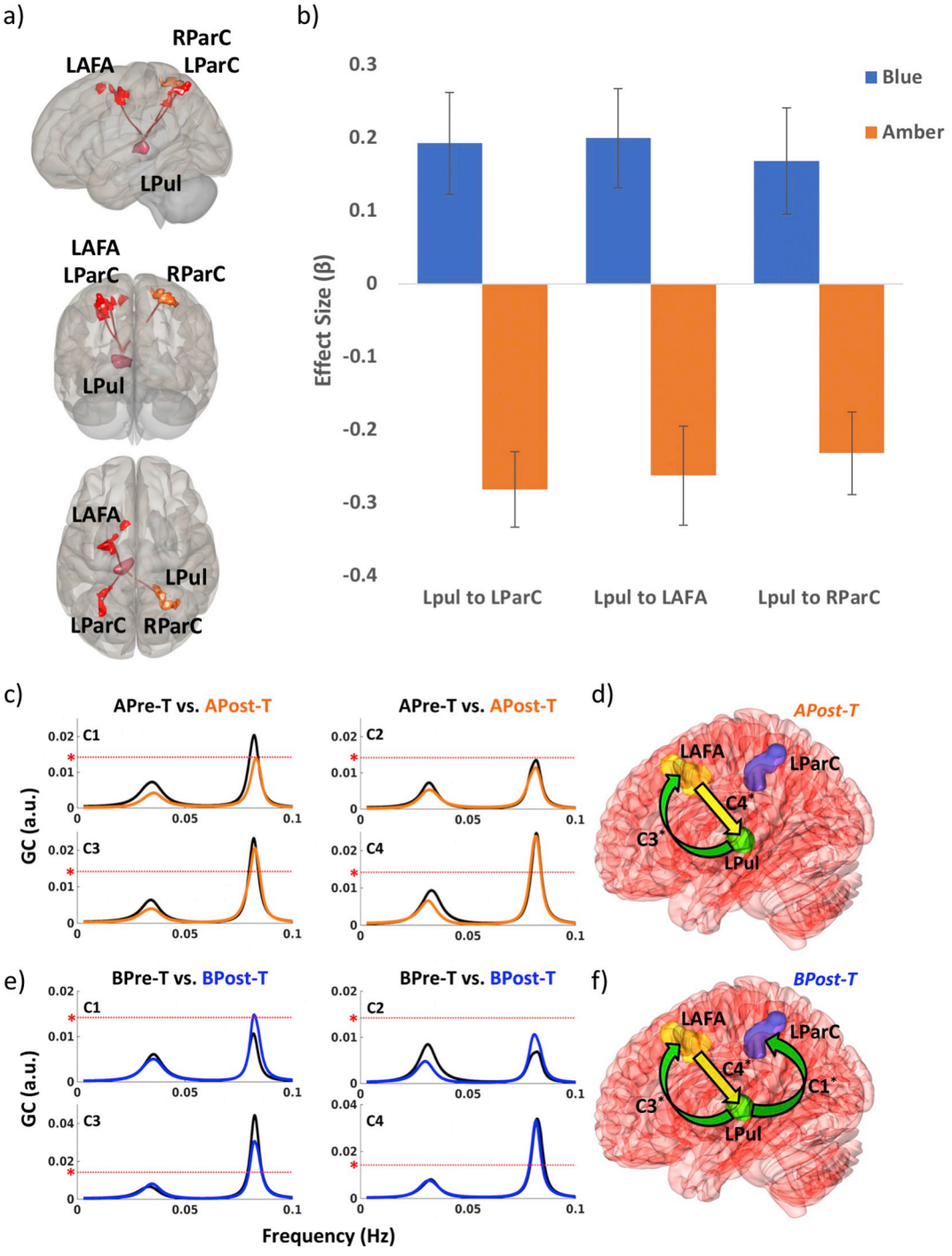

Fig. 7. Functional Connectivity (FC) and Granger causality measures. (a) The extracted volumes from the VBM analysis were used to investigate the main effect on FC associated with the observed structural changes in the left thalamic (LPul) and right thalamic (RPul) regions. Individual subject seed-to-voxel whole brain connectivity maps identified three clusters of voxels associated with significant increases in connectivity to the LPul. The extracted clusters (i.e. Left Parietal Cortex: LParC, Left Agranular Frontal Area: LAFA, and the Right Parietal Cortex: RParC), are plotted in the figures for visualization with the strength of the correlation represented by the colour of the line. (b) The resting-state correlations for FC between the LPul and ROIs were extracted as beta weights for each participant and the correlation is plotted for the BLUE and AMBER groups separately with error bars representing the within-group standard errors. (c-f) Next we show that the peaks from GC-frequency spectra are at frequency $<$ 0.1 Hz for the directed connectivity from the LPul to LParC (C1), LParC to LPul (C2), LPul to LAFA (C3), and LAFA to LPul (C4) for both ALT group (c-d) (Pre-treatment: APre-T and Post-treatment: APost-T), and BLT group (e-f) (Pre-treatment: BPre-T and Post-treatment: BPost-T). Dotted lines represent the threshold value of GC estimated from the permutation test at p £10^{-4}. Overall, GC measures between LPul and LAFA (C3 and C4) for APost-T (e) and between LPul and LAFA (C3 and C4) as well as from LPul to LParC (C1) for BPost-T (f) showed significant directional influence. (For interpretation of the references to colour in this figure legend, the reader is referred to the web version of this article.)

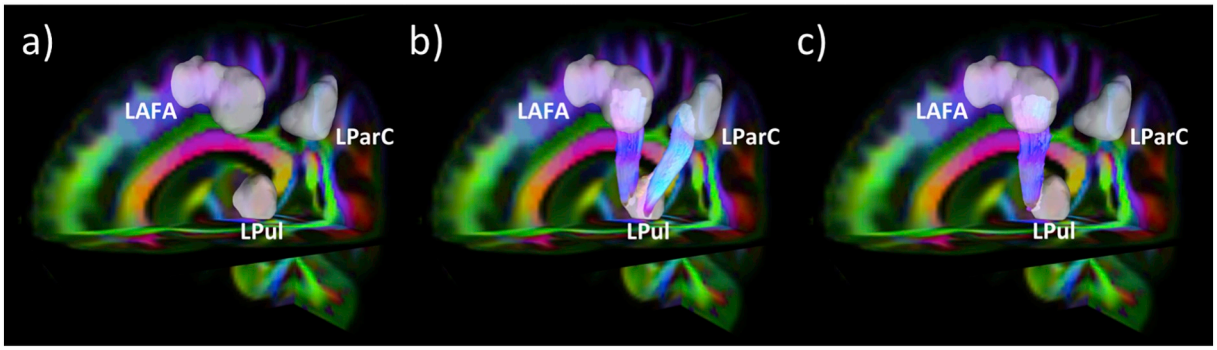

Fig. 8. Diffusion connectometry analysis for amber-light treatment (ALT) and blue-light treatment (BLT) groups. We found that there were no tracts with significant differences between pre- and post-treatment conditions for fractional anisotropy (FA) (FDR $>$ 0.05) in either ALT or BLT group (a). However, we found tracts connecting LPul and LParC with significant reduction in isotropic diffusion (ISO) following treatment for BLT group (b) (FDR $<$ 0.05), but not for ALT group (FDR $>$ 0.05). Also, there were tracts connecting LPul and LAFA with reduced ISO following treatment for BLT group (FDR = 0.11) (c) and a significant increase in ISO following treatment for ALT group (FDR $<$ 0.05) (c). Here, identified tracts are colour-coded in transverse (right-left: red), longitudinal (anterior-posterior: green) and horizontal (foot-head: blue) directions and overlaid on colour-coded FA image. (For interpretation of the references to colour in this figure legend, the reader is referred to the web version of this article.)

associated with a significant improvement in the completion speed of each move. Moreover, participants in the BLUE light condition also made more correct moves per unit of time, suggesting greater efficiency in planning and execution when compared to those in the placebo group. To our knowledge, this is the first study to examine the effects of daily blue-wavelength light exposure on executive function tasks that incorporate planning and sequencing ability. Further research will be necessary to determine the extent and nature of neurocognitive changes produced by daily exposure to blue light in the morning.

While prior research suggests an association between regular exposure to blue light in the early waking hours and reduced fatigue and sleepiness in patients with TBI (Sinclair et al., 2014), the underlying neurobiological mechanisms contributing to these effects have remained unclear. Recently, Clark and colleagues demonstrated that fatigue following mTBI was explicitly associated with reduced thalamic volume (Clark et al., 2018). We found that the BLUE light intervention was associated with a significant increase in GMV of the mediodorsal and pulvinar regions of the thalamus bilaterally compared to the AMBER light condition. Some studies suggest that the thalamus is particularly vulnerable to the disruptive effects of mTBI (Bolzenius et al., 2018; Naess-Schmidt et al., 2017), perhaps due to its centralized location and extensive anatomical/functional connectivity. Furthermore, increases in mean thalamic volume correlate with the recovery of cognitive performance in individuals with mTBI (Munivenkatappa et al., 2016). Sleep loss is associated with decreased thalamic volumes, suggesting a potential role for sleep in modulating the volume of the thalamus (Dai et al., 2018; Liu et al., 2014). Our findings suggest that alterations in circadian rhythms or improvements in sleep secondary to daily blue light exposure may contribute to the observed structural changes and associated performance outcomes in this study.

The BLUE light condition was associated with increased functional connectivity between the left thalamus and cortical regions in the frontal and parietal cortex, relative to the AMBER condition, and this change correlated with improvements in daytime sleepiness, language performance, and executive functioning. This effect is consistent with prior research showing negative correlations in thalamocortical functional connectivity and fatigue in patients with mTBI (Nordin et al., 2016). Compared to non-injured controls, patients with mTBI have decreased functional connectivity between the thalamus and cortical regions including the dorsal attention network and the frontoparietal control network (Banks et al., 2016). Moreover, these patterns of disrupted connectivity tend to attenuate throughout recovery, with positive associations between symptom improvement and increases in connectivity across these networks (Banks et al., 2016). Our findings suggest that daily morning exposure to blue-wavelength light may help facilitate the dynamic relationship between the restoration of connectivity with cognitive and symptom recovery.

Finally, we examined whether the increases in the structural connectivity of axonal pathways secondary to the intervention were associated with changes in neurocognitive performance. Prior research in patients with mTBI demonstrates reductions in white matter anisotropy between the left thalamus and prefrontal regions in patients with mTBI (Aoki and Inokuchi, 2016). Our findings suggest that blue light treatment may facilitate the reversal of some of these deficits, as we found increased structural integrity in axonal tracts connecting the left thalamus to the left prefrontal and left parietal cortex after blue light treatment. Moreover, the magnitude of increases in the structural integrity of these pathways correlated with improved neuropsychological performances, particularly those involving visual construction and delayed memory abilities. We propose that the post-treatment decreases in isotropic diffusion for these tracts may reflect increased myelination, due to the proliferation of oligodendrocyte precursor cells that have been previously shown to be enhanced by sleep (Bellesi et al., 2013). Future research will be necessary to verify this assertion.

Several methodological limitations should be kept in mind. These include modest capacity to monitor treatment compliance, lack of experimental control over the direction of gaze when using the light device, and the use of wrist actigraphy as a proxy for gold-standard nightly polysomnographic sleep recordings. Further, we also found that half of the participants reported experiencing more than one lifetime concussion. Unfortunately, we did not collect data on the time frame between multiple concussions, which is also a limitation. Finally, the present analysis only focused on primary outcome variables collected at baseline and after 6-weeks of treatment. Forthcoming work will explore actigraphic variables in depth at each week to determine whether sleep outcomes reach their peak before 6-weeks. With due consideration to these limitations, we believe that the present findings provide compelling evidence for the role of sleep and circadian systems in brain repair and suggest that stimulation of the ipRGC-SCN system, via daily exposure to morning blue-wavelength light, may offer an effective method for re-entraining the circadian system and facilitating recovery among individuals with a recent mTBI.

Acknowledgments

This study was funded by a grant from the U.S. Army Medical Research and Development Command (W81XWH-11-1-0056) to W.D.S.K.

References

Aoki, Y., Inokuchi, R., 2016. A voxel-based meta-analysis of diffusion tensor imaging in mild traumatic brain injury. Neurosci. Biobehav. Rev. 66, 119–126.

Arendt, J., 2006. Melatonin and human rhythms. Chronobiol. Int. 23, 21–37.

Bajaj, S., et al., 2016. Bridging the gap: dynamic causal modeling and granger causality analysis of resting state functional magnetic resonance imaging. Brain Connect. 6, 652–661.

Bajaj, S., et al., 2017. Blue-light therapy following mild traumatic brain injury: effects on white matter water diffusion in the brain. Front. Neurol. 8, 616.

Banks, S.D., et al., 2016. Thalamic functional connectivity in mild traumatic brain injury: longitudinal associations with patient-reported outcomes and neuropsychological tests. Arch. Phys. Med. Rehabil. 97, 1254–1261.

Beck, A.T., et al., 1996. BDI-II: Beck Depression Inventory Manual. Psychological Corporation, San Antonio, TX.

Bellesi, M., et al., 2013. Effects of sleep and wake on oligodendrocytes and their precursors. J. Neurosci. 33, 14288–14300.

Bellesi, M., et al., 2016. Contribution of sleep to the repair of neuronal DNA double-strand breaks: evidence from flies and mice. Sci. Rep. 6, 36804.

Bellesi, M., et al., 2018. Myelin modifications after chronic sleep loss in adolescent mice. Sleep. 41.

Blair, R.C., Karniski, W., 1993. An alternative method for significance testing of waveform difference potentials. Psychophysiology. 30, 518–524.

Bolzenius, J.D., et al., 2018. Relationships between subcortical shape measures and subjective symptom reporting in US Service members with mild traumatic brain injury. J. Head Trauma Rehabil. 33, 113–122.

Brovelli, A., et al., 2004. Beta oscillations in a large-scale sensorimotor cortical network: directional influences revealed by granger causality. Proc. Natl. Acad. Sci. U. S. A. 101, 9849–9854.

Cajochen, C., et al., 2003. Role of melatonin in the regulation of human circadian rhythms and sleep. J. Neuroendocrinol. 15, 432–437.

Clark, A.L., et al., 2018. Fatigue is associated with global and regional thalamic morphometry in veterans with a history of mild traumatic brain injury. J. Head Trauma Rehabil. 33, 382–392.

Cordes, D., et al., 2001. Frequencies contributing to functional connectivity in the cerebral cortex in “resting-state” data. AJNR Am. J. Neuroradiol. 22, 1326–1333.

Dai, X.J., et al., 2018. Plasticity and susceptibility of brain morphometry alterations to insufficient sleep. Front Psychiatry. 9, 266.

de Vivo, L., et al., 2017. Ultrastructural evidence for synaptic scaling across the wake/sleep cycle. Science. 355, 507–510.

Dhamala, M., 2013. Spectral interdependency methods. In: Jaeger, D., Jung, R. (Eds.), Encyclopedia of Computational Neuroscience. Springer New York, New York, NY.

Dhamala, M., et al., 2008a. Analyzing information flow in brain networks with nonparametric granger causality. Neuroimage. 41, 354–362.

Dhamala, M., et al., 2008b. Estimating granger causality from fourier and wavelet transforms of time series data. Phys. Rev. Lett. 100, 018701.

Dinges, D.F., Powell, J.W., 1985. Microcomputer analyses of performance on a portable, simple, visual RT task during sustained operations. Behav. Res. Methods Instrum. Comput. 17, 652–655.

Durmer, J.S., Dinges, D.F., 2005. Neurocognitive consequences of sleep deprivation. Semin. Neurol. 25, 117–129.

Figueiro, M.G., et al., 2014. Tailored lighting intervention improves measures of sleep, depression, and agitation in persons with Alzheimer’s disease and related dementia living in long-term care facilities. Clin. Interv. Aging 9, 1527–1537.

Gao, B., et al., 2010. Sleep disruption aggravates focal cerebral ischemia in the rat. Sleep. 33, 879–887.

Geerdink, M., et al., 2016. Short blue light pulses (30 min) in the morning support a sleep-advancing protocol in a home setting. J. Biol. Rhythm. 31, 483–497.

Gilbert, K.S., et al., 2015. Sleep disturbances, TBI and PTSD: implications for treatment and recovery. Clin. Psychol. Rev. 40, 195–212.

Grima, N.A., et al., 2016. Circadian melatonin rhythm following traumatic brain injury. Neurorehabil. Neural Repair 30, 972–977.

VA/DoD Management of Concussion/mTBI Working Group, 2009. VA/DoD clinical practice guidelines for maagement of concussion/mild traumatic brain injury. J. Rehabil. Res. Dev. 46, CP1–68.

Hattar, S., et al., 2002. Melanopsin-containing retinal ganglion cells: architecture, projections, and intrinsic photosensitivity. Science. 295, 1065–1070.

Herscovitch, J., Broughton, R., 1981. Sensitivity of the stanford sleepiness scale to the effects of cumulative partial sleep deprivation and recovery oversleeping. Sleep. 4, 83–91.

Honma, S., 2018. The mammalian circadian system: a hierarchical multi-oscillator structure for generating circadian rhythm. J. Physiol. Sci. 68, 207–219.

Johns, M.W., 1991. A new method for measuring daytime sleepiness: the Epworth sleepiness scale. Sleep. 14, 540–545.

Killgore, W.D.S., et al., 2006. Impaired decision-making following 49 hours of sleep deprivation. J. Sleep Res. 15, 7–13.

Killgore, W.D.S., et al., 2007. The effects of 53 hours of sleep deprivation on moral judgment. Sleep. 30, 345–352.

King, P.R., et al., 2012. Psychometric study of the neurobehavioral symptom inventory. J. Rehabil. Res. Dev. 49, 879–888.

Lavie, P., 2001. Sleep-wake as a biological rhythm. Annu. Rev. Psychol. 52, 277–303.

Liu, C., et al., 2014. Long-term total sleep deprivation reduces thalamic gray matter volume in healthy men. Neuroreport. 25, 320–323.

Marino, M., et al., 2013. Measuring sleep: accuracy, sensitivity, and specificity of wrist actigraphy compared to polysomnography. Sleep. 36, 1747–1755.

Monk, T.H., 2005. The post-lunch dip in performance. Clin. Sports Med. 24 (e15–23), xi–xii.

Munivenkatappa, A., et al., 2016. Role of the thalamus in natural recovery of cognitive impairment in patients with mild traumatic brain injury. Brain Inj. 30, 388–392.

Naess-Schmidt, E.T., et al., 2017. Microstructural changes in the thalamus after mild traumatic brain injury: a longitudinal diffusion and mean kurtosis tensor MRI study. Brain Inj. 31, 230–236.

Nordin, L.E., et al., 2016. Post mTBI fatigue is associated with abnormal brain functional connectivity. Sci. Rep. 6, 21183.

Oldfield, R.C., 1971. The assessment of handedness: the Edinburgh inventory. Neuropsychologia. 9, 97–111.

Orff, H.J., et al., 2009. Traumatic brain injury and sleep disturbance: a review of current research. J. Head Trauma Rehabil. 24, 155–165.

Panda, S., et al., 2002. Melanopsin (Opn4) requirement for normal light-induced circadian phase shifting. Science. 298, 2213–2216.

Panda, S., et al., 2005. Illumination of the melanopsin signaling pathway. Science. 307, 600–604.

Provencio, I., et al., 2000. A novel human opsin in the inner retina. J. Neurosci. 20, 600–605.

Qiu, X., et al., 2005. Induction of photosensitivity by heterologous expression of melanopsin. Nature. 433, 745–749.

Raikes, A.C., Killgore, W.D., 2018. Potential for the development of light therapies in mild traumatic brain injury. Concussion. 3, CNC57.

Rao, V., et al., 2008. Prevalence and types of sleep disturbances acutely after traumatic brain injury. Brain Inj. 22, 381–386.

Richardson, C., et al., 2018. A randomised controlled trial of bright light therapy and morning activity for adolescents and young adults with delayed sleep-wake phase disorder. Sleep Med. 45, 114–123.

Rorden, C., et al., 2007. Improving lesion-symptom mapping. J. Cogn. Neurosci. 19, 1081–1088.

Rosa, J.P.P., et al., 2018. Effect of bright light therapy on delayed sleep/wake cycle and reaction time of athletes participating in the Rio 2016 Olympic games. Chronobiol. Int. 35, 1095–1103.

Sapede, D., Cau, E., 2013. The pineal gland from development to function. Curr. Top. Dev. Biol. 106, 171–215.

Saxvig, I.W., et al., 2014. A randomized controlled trial with bright light and melatonin for delayed sleep phase disorder: effects on subjective and objective sleep. Chronobiol. Int. 31, 72–86.

Sheehan, D.V., et al., 1998. The Mini-International Neuropsychiatric Interview (M.I.N.I.): the development and validation of a structured diagnostic psychiatric interview for DSM-IV and ICD-10. J. Clin. Psychiatry 59 (Suppl. 20), 22–33 (quiz 34–57).

Shekleton, J.A., et al., 2010. Sleep disturbance and melatonin levels following traumatic brain injury. Neurology. 74, 1732–1738.

Sinclair, K.L., et al., 2014. Randomized controlled trial of light therapy for fatigue following traumatic brain injury. Neurorehabil. Neural Repair 28, 303–313.

Sullivan, K.A., et al., 2016. Poor sleep predicts subacute postconcussion symptoms following mild traumatic brain injury. Appl Neuropsychol. Adult. 23, 426–435.

Tahkamo, L., et al., 2018. Systematic review of light exposure impact on human circadian rhythm. Chronobiol. Int. 1–20.

Tononi, G., Cirelli, C., 2014. Sleep and the price of plasticity: from synaptic and cellular homeostasis to memory consolidation and integration. Neuron. 81, 12–34.

Tucker, A.M., et al., 2010. Effects of sleep deprivation on dissociated components of executive functioning. Sleep. 33, 47–57.

Tzourio-Mazoyer, N., et al., 2002. Automated anatomical labeling of activations in SPM using a macroscopic anatomical parcellation of the MNI MRI single-subject brain. Neuroimage. 15, 273–289.

Verma, A., et al., 2007. Sleep disorders in chronic traumatic brain injury. J. Clin. Sleep Med. 3, 357–362.

Whitfield-Gabrieli, S., Nieto-Castanon, A., 2012. Conn: a functional connectivity toolbox for correlated and anticorrelated brain networks. Brain Connectivity. 2, 125–141.

Woo, C.W., et al., 2014. Cluster-extent based thresholding in fMRI analyses: pitfalls and recommendations. Neuroimage. 91, 412–419.

Wu, L.M., et al., 2018. The effect of systematic light exposure on sleep in a mixed group of fatigued cancer survivors. J. Clin. Sleep Med. 14, 31–39.

Xie, L., et al., 2013. Sleep drives metabolite clearance from the adult brain. Science. 342, 373–377.

Yeh, F.C., Tseng, W.Y., 2011. NTU-90: a high angular resolution brain atlas constructed by q-space diffeomorphic reconstruction. Neuroimage. 58, 91–99.

Yeh, F.C., et al., 2013. Deterministic diffusion fiber tracking improved by quantitative anisotropy. PLoS One 8, e80713.

Yeh, F.C., et al., 2016. Connectometry: a statistical approach harnessing the analytical potential of the local connectome. Neuroimage. 125, 162–171.

Zunzunegui, C., et al., 2011. Sleep disturbance impairs stroke recovery in the rat. Sleep. 34, 1261–1269.